Article

Current Biology

Nest Carbon Dioxide Masks GABA-Dependent Seizure Susceptibility in the Naked Mole-Rat

Highlights

- Eusocial African naked mole-rats raise colony-nest CO_2 to anticonvulsant levels
- Naked mole-rats harbor an epilepsy-related variant in neuronal Cl^- extruder KCC2
- GABA-acting antiseizure drug diazepam triggers seizures in naked mole-rats
- Diazepam is rendered seizure-suppressing in nest-like levels of CO_2 in inhaled air

Authors

Michael Zions, Edward F. Meehan, Michael E. Kress, ..., Kai Kaila, Martin Puskarjov, Dan P. McCloskey

Correspondence

martin.puskarjov@gmail.com (M.P.), dan.mccloskey@csi.cuny.edu (D.P.M.)

In Brief

Zions et al. show a dependence of captive naked mole-rats on elevated carbon dioxide (CO_2) in the colony nest to avoid seizure. They also show a species-specific mutation of the cation-chloride cotransporter KCC2, compromising neuronal Cl^- extrusion. Evolution may have favored selection of this energy-saving mutation, which is masked by the anticonvulsant properties of CO_2.

Zions et al., 2020, Current Biology *30*, 2068–2077
June 8, 2020
https://doi.org/10.1016/j.cub.2020.03.071

CellPress

CellPress
OPEN ACCESS

Current Biology

Article

Nest Carbon Dioxide Masks GABA-Dependent Seizure Susceptibility in the Naked Mole-Rat

Michael Zions,[1,2] Edward F. Meehan,[3,4] Michael E. Kress,[4,5] Donald Thevalingam,[1,2] Edmund C. Jenkins,[2] Kai Kaila,[6,7] Martin Puskarjov,[2,7,*] and Dan P. McCloskey[1,2,3,8,*]

[1]PhD Program in Neuroscience, Graduate Center of The City University of New York, New York, NY 10016, USA
[2]Center for Developmental Neuroscience, College of Staten Island in the City University of New York, Staten Island, NY 10314, USA
[3]Department of Psychology, College of Staten Island in the City University of New York, Staten Island, NY 10314, USA
[4]Department of Computer Science, College of Staten Island in the City University of New York, Staten Island, NY 10314, USA
[5]PhD Program in Computer Science, Graduate Center of the City University of New York, New York, NY 10016, USA
[6]Neuroscience Center (HiLIFE), University of Helsinki, Helsinki, Finland
[7]Molecular and Integrative Biosciences, Faculty of Biological and Environmental Sciences, University of Helsinki, Helsinki, Finland
[8]Lead Contact
*Correspondence: martin.puskarjov@gmail.com (M.P.), dan.mccloskey@csi.cuny.edu (D.P.M.)
https://doi.org/10.1016/j.cub.2020.03.071

SUMMARY

African naked mole-rats were likely the first mammals to evolve eusociality, and thus required adaptations to conserve energy and tolerate the low oxygen (O_2) and high carbon dioxide (CO_2) of a densely populated fossorial nest. As hypercapnia is known to suppress neuronal activity, we studied whether naked mole-rats might demonstrate energy savings in GABAergic inhibition. Using whole-colony behavioral monitoring of captive naked mole-rats, we found a durable nest, characterized by high CO_2 levels, where all colony members spent the majority of their time. Analysis of the naked mole-rat genome revealed, uniquely among mammals, a histidine point variation in the neuronal potassium-chloride cotransporter 2 (KCC2). A histidine missense substitution mutation at this locus in the human ortholog of KCC2, found previously in patients with febrile seizures and epilepsy, has been demonstrated to diminish neuronal Cl^- extrusion capacity, and thus impairs GABAergic inhibition. Seizures were observed, without pharmacological intervention, in adult naked mole-rats exposed to a simulated hyperthermic surface environment, causing systemic hypocapnic alkalosis. Consistent with the diminished function of KCC2, adult naked mole-rats demonstrate a reduced efficacy of inhibition that manifests as triggering of seizures at room temperature by the $GABA_A$ receptor ($GABA_AR$) positive allosteric modulator diazepam. These seizures are blocked in the presence of nest-like levels of CO_2 and likely to be mediated through $GABA_AR$ activity, based on *in vitro* recordings. Thus, altered GABAergic inhibition adds to a growing list of adaptations in the naked mole-rat and provides a plausible proximate mechanism for nesting behavior, where a return to the colony nest restores GABA-mediated inhibition.

INTRODUCTION

Eusociality, a system of extreme reproductive altruism, has evolved only twice in vertebrates, both times in fossorial mole-rats, as proposed initially by Richard Alexander in 1974 [1, 2]. Of the two eusocial mole-rat species, the more reproductively skewed eusocial African naked mole-rat is believed to have evolved first, around 35 million years ago [3]. Unlike other vertebrates, mature naked mole-rats rarely disperse from their natal colony but participate in a caste system with overlapping adult generations cooperating in foraging, brood care, and maintenance and defense of the colony nest [4]. The transition to eusociality in this species appeared to occur not long after it became fossorial, which served as a successful adaptation to thrive in the predator-rich and patchy food conditions of semi-arid sub-Saharan Africa. As members of the Bathyergidae family, African mole-rats range from solitary to eusocial within similar environmental niches. It is clear that the emergence of eusociality in the naked mole-rat is an adaptation to enhance evolutionary fitness, rather than a constraint.

The rarity of eusociality among mammals underscores the challenges posed by such an adaptation. The largest challenge is likely to be overcoming the high energy costs required by mammals compared to invertebrates. A durable and defensible centralized colony nest appears to be a universal feature of eusocial species [5], yet a densely occupied underground nest in naked mole-rats—the species with the largest colony size (up to 300 individuals) of any mammal [6]—limits access to O_2 and food. Naked mole-rats have successfully reduced energy demand and increased efficiency behaviorally through cooperative foraging [7], thermoregulation (huddling) [8, 9], and physiologically through adaptations including lowered metabolic rate [9–11], enhanced O_2 delivery to organs [12–14], and remarkable alternative metabolic strategies to address hypoxia [15].

Huddling in the naked mole-rat nest is achieved due to the permissive fossorial environment, which buffers the wide daily and seasonal excursions measured aboveground to stable temperatures at the deeper parts of the burrow, likely to house the colony nest [6, 16, 17]. These areas are cooler (19°C–28°C)

[16] than the range of naked mole-rat thermoneutrality (31°C–34°C) [8]. When naked mole-rats huddle at thermoneutral temperatures, O_2 consumption and metabolic demand decrease as group size increases [9]. This is likely due to the unique lack of a hypercapnia-triggered increase in ventilation in this species [18], achieved, in part, through diminished substance P signaling [19]. Therefore, large-group huddles in the cool colony nest may be particularly advantageous for both thermoregulation and energy conservation.

The most accurate estimates of naked mole-rat burrow air composition to date show only mildly elevated levels of CO_2 (0.4%) in unoccupied or low occupied areas [16], well within the range of what has been reported for other fossorial mammalian species [20]. It is clear, however, from a number of experimental studies that naked mole-rats have adapted to tolerate elevated CO_2 levels. These adaptations include prolonged survival even in extreme hypercapnia [15], the lack of typical behavioral and respiratory responses to elevated ambient CO_2 levels [15, 21–23], a decreased CO_2 sensitivity of neuronal gap junctions [24], and an insensitivity to certain acidic stimuli [25–27].

These adaptations, along with lower than expected adult brain volume [28] and neuron number [29] likely reflect the naked mole-rat's ability to restrict energy consumption by the brain, the most energy-demanding organ in the body [30]. The naked mole-rat colony nest may create a permissive environment for brain energy savings through hypercapnia, which has been shown to diminish neuronal activity in rodents [31], non-human primates [32], and humans [33]. The potent anticonvulsant action of CO_2 in rodents and humans [34, 35] is in line with the fact that hypercapnia suppresses neural excitability. Thus, we hypothesize that maintaining the brain in a chronic hypercapnic state establishes a positive selection pressure for gene variants that save energy by eliminating other mechanisms to maintain inhibitory tone. While such variants might lead to seizures and lowered fitness in a normocapnic environment, they may increase fitness through lowered metabolic need under hypercapnia.

The mammalian brain works close to theoretical limits on energy consumption, with most of it used to maintain the ionic driving forces that are needed for electrical signaling [30]. Changes in the functions and expression patterns of ion channels and transporters may thus have evolved in the naked mole-rat to protect neurons during states of energy crisis. An important energy-demanding process in the mammalian brain is the extrusion of intraneuronal Cl^- by the KCC2 cation-chloride cotransporter [36]. As a secondary-active transporter, KCC2 indirectly expends ATP to extrude Cl^- via energy stored in the K^+ gradient generated by the Na-K ATPase [37]. KCC2 is typically downregulated under energy crises [36] and inhibition of cation-chloride cotransport enhances ATP recovery following oxygen-glucose deprivation [38]. In typical mammals, the ability of GABA to hyperpolarize neurons and inhibit their activity depends upon the developmental up-regulation of KCC2, leading to lowered intraneuronal Cl^- concentration [37]. Improper function of KCC2 can impair GABAergic signaling and has been implicated in seizure and neurodevelopmental disorders such as epilepsy, autism, and schizophrenia [39–46].

Here, we monitored whole-colony behavior of captive naked mole-rats and found that these animals consistently established a colony nest. Each colony member spent the majority of their time in the nest, which was measured to have elevated CO_2 levels. Notably, naked mole-rats demonstrated a vulnerability to hypocapnic alkalosis, which manifests as seizures in environments that mimic the aboveground conditions in their native habitat. Analysis of the naked mole-rat genome revealed a species-specific histidine point variant in exon 22, a highly conserved regulatory region of KCC2 [47, 48]. This variation has also been identified in humans with febrile seizures, idiopathic generalized epilepsy, autism spectrum disorder, and schizophrenia, in contrast to the general population carrying an arginine at this position [41, 43, 44]. Apart from the naked mole-rat, the only other species across Mammalia without an arginine at this locus is the only other eusocial mammal, the Damaraland mole-rat, which carries a cysteine.

Consistent with diminished function of KCC2, naked mole-rats demonstrate reduced efficacy of GABAergic inhibition, which, remarkably, manifests as the triggering of seizures in adult naked mole-rats at room temperature by the GABAergic positive allosteric modulator diazepam. These seizures are blocked or reversed in the presence of nest-like levels of CO_2 and are likely to be mediated through $GABA_AR$ activity, based on *in vitro* recordings. We propose that naked mole-rats have adapted a diminished GABAergic inhibitory tone as an energy-saving mechanism due to the permissive neuromodulatory conditions of the high CO_2 colony nest, thus establishing the nest as an important attractor for animal activity.

RESULTS

Captive naked mole-rats housed in an environment with multiple interconnected chambers demonstrated a prominent nest in each colony, with the nest location determined by colony members. The implantation of whole colonies with passive radio frequency identification (RFID) transponders and the positioning of antennas around the housing environment [49] showed a highly conserved space utilization, with the majority of activity concentrated around a single nest chamber, with the location of the nest chamber changing periodically (Figure 1A). Tracking the activity of individual colony members showed that all individuals of the colony remained in the nest, huddling [50], with forays to the food chamber and specific chambers designated by the colony as toilet chambers. Regardless of caste (reproductive, large worker, small worker) or time of day, even when measured over long time periods, all individuals spent a large proportion of time in the nest chamber (more than 70%, averaged over 26 days and across two colonies), with the queen and breeding male of each colony showing the highest proportion of time in the nest (Figure 1B). Visual representations of the individual naked mole-rat and chamber locations confirmed the nest as a focus of colony behavior over weeks of measurement (Video S1).

Measurements of CO_2 from a total of 96 chambers in the occupied housing environments of five different naked mole-rat colonies showed a steep gradient from the nest to non-nest areas with a minimum recorded value of 0.05% (of volume) in a toilet chamber, and a maximum recorded value of 2.33% in a nest chamber, which is considerably higher than the highest levels recorded in non-nest portions of the burrow in the wild [16]. The nest chamber of each colony consistently showed the highest CO_2 levels (1.15% ± 0.41%, n = 8), followed by the

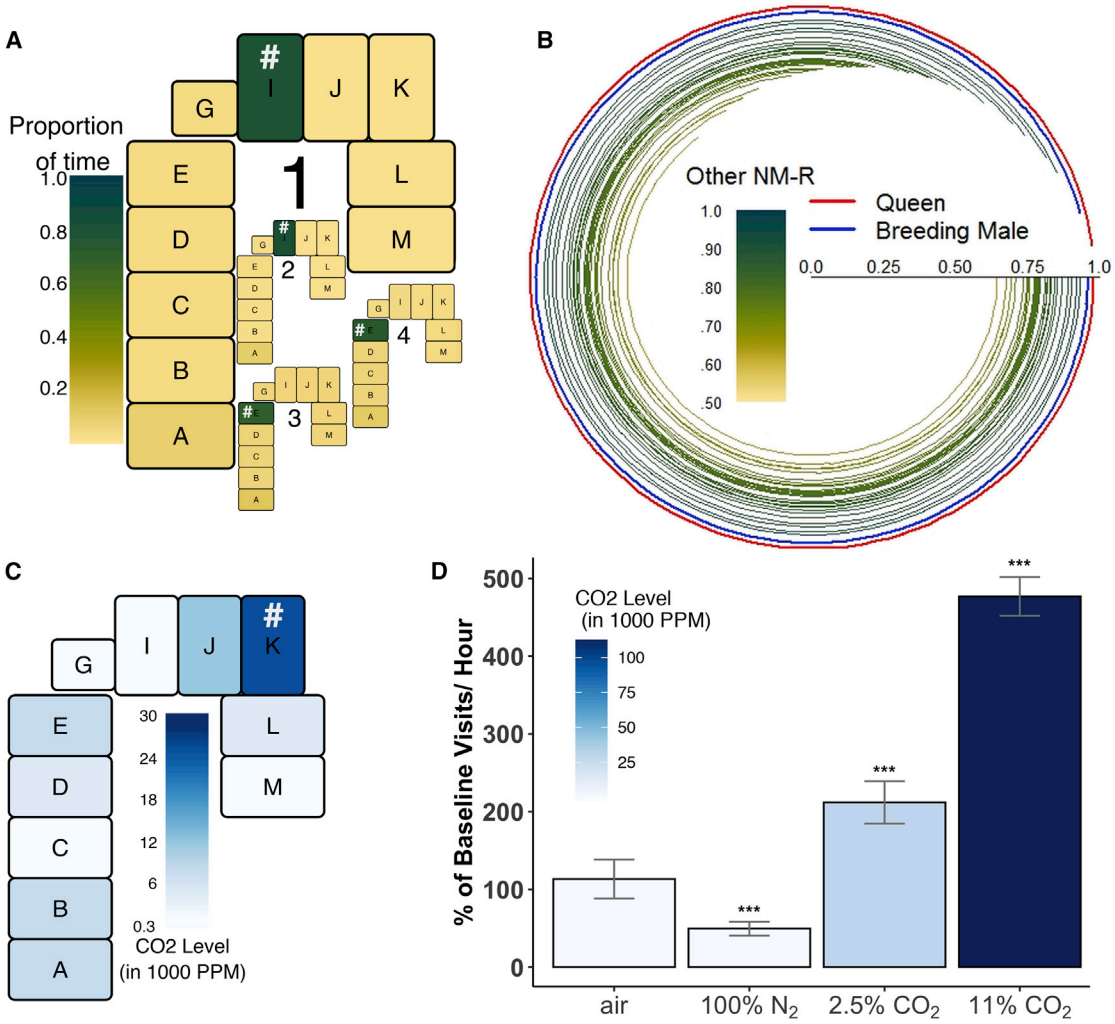

Figure 1. Colony Behavior of Naked Mole-Rats Shows Preference for High CO_2 Environments

(A) Radio frequency identification (RFID)-measured proportion of time spent in each of 11 colony chambers in the laboratory housing environment of colony TT-2 over four 60-h periods (consecutive weekends with no human intervention). See Video S1 for an overview of hourly activity. Note the high concentration of animals in chamber "I" for the first two periods and chamber "E" for the third and fourth periods, indicating the relocation of the colony nest. #Location of the colony nest during each period.

(B) Proportion of time spent at the colony-nest location (determined based on the location of the majority of colony members at any given hour) for each of the 36 members of the TT-2 colony over a 26-day period, which includes the four periods identified in (A). Colors of individual lines represent the proportion of time spent in the nest for each animal and is based on the scale provided in (A). The colony queen is indicated by a red line, and the breeding male is indicated by a blue line.

(C) Chamber air CO_2 levels for each of the chambers in colony TT-2 collected with a minimum of three samples per chamber over a 14-day period. Note that the nest location was consistently in chamber "K" during this collection period, as indicated by #.

(D) Activity at test chamber RFID antennas during exposure to compressed room air (air; 0.04% CO_2), pure N_2, or two levels of highly elevated CO_2. Exogenously delivered gases were infused into a non-nest chamber in two different colonies, and the activity at RFID antennas was quantified. See Figure S1 for an example of colony-nest movement during a gas infusion experiment. ***$p < 0.001$ to baseline levels (100), one-way ANOVA with Bonferroni-adjusted pairwise comparison.

chamber where food was placed each day (0.49 ± 0.13%, n = 5). Figure 1C shows the housing environments for the TT-2 colony with average CO_2 values recorded per chamber. Thus, our results suggest that naked mole-rats spend the majority of their time in the most CO_2-rich areas of the housing environment, despite protection and equivalent temperature elsewhere in the housing environment.

To determine whether naked mole-rats tolerate or prefer the hypercapnia experienced in the nest chamber, we measured the amount of activity in a non-nest chamber in the same housing environment infused with exogenous CO_2. Following a 24-h baseline period, CO_2, compressed room air (containing 0.04% CO_2), or pure nitrogen gas (N_2) was infused into the test chamber. High CO_2 levels levels comprising 2.5% or 11% were tested and run in two separate experiments with different colonies and housing arrangements. When the level of RFID activity at the entrances to the gas infusion chambers was measured, we found significant increases in the frequency of visits when CO_2 was infused but not when the gas infused was room air or pure N_2 (Figure 1D).

The effect of CO_2 infusion on nesting behavior was also examined by monitoring the influence of gas application to the existing colony environment on nest location in the colony. Figure S1 shows the proportion of time spent by animals in the TT-2 colony in one of three observed nesting locations (chambers G and K—typical nesting locations; and chamber M—a location that was not previously used as a colony nest). Nesting in the test chamber M was monitored through a 24-h baseline period, a 24-h CO_2 infusion period, a 71-h recovery period, a 5-h N_2 infusion period (set to return CO_2 to 0.1%), and a second 71-h recovery period. During the baseline period, an average of 6.5% ± 0.8% of animals nested in chamber M during any given hour, with the majority of animals nesting in chamber G (83.1% ± 1.41%). Nesting in chamber M increased slightly from baseline (8.4% ± 2.0%) during the period of CO_2 infusion. When the CO_2 infusion was turned off, nesting in chamber M increased to 40.8% ± 4.3%, establishing the nest in this chamber for the first time and reaching the highest percentage of nesting animals for any of the three nests (98.4%) during hour 57 of recovery. Conducting a similar routine in a third colony (L-1), under video surveillance, showed the movement of the nest to a chamber adjacent to the gas infusion chamber during infusion of 2.5% CO_2.

Pure N_2 gas was infused into chamber M (at a rate identical to the rate of CO_2 infusion), lowering chamber M CO_2 values to baseline (0.01%). During this period, the animals exited chamber M and moved the nest to chamber K, reducing the percentage of animals in chamber M to 11.9% ± 3.1% for this period. This part of the experiment, which was planned to run for 24 h, was discontinued after 5 h when animals were found deceased in chamber L, near the entrance to chamber M. During the next recovery period, the nest was maintained in chamber K (60.2% ± 2.6% of animals), with an average of 8.2% of animals located in chamber M during this period.

Using a Bayesian structural time-series model, we assessed the impact that these experimental manipulations had on the activity patterns in the test chamber. Figure S1 shows an overlay of the actual activity data along with the predicted activity, which was derived from the 24-h baseline period. The model yielded a significant impact of the experimental manipulation overall (Bayesian one-sided tail area probability: $p = 0.001$), with the CO_2 recovery, N_2 infusion, and N_2 recovery all showing a significant increase from the activity levels predicted by the model ($p < 0.0125$, Bonferroni-corrected). Taken together, our results show that high CO_2, but not other exogenous gases tested, cause an increase in visits and nesting behavior in a part of the housing environment that is not commonly visited and does not typically house the colony nest. Animals build nests adjacent to the infusion chamber during CO_2 infusion and into the infusion chamber after CO_2 is turned off, indicating a preference for the higher CO_2 areas of the housing environment.

Naked mole-rat activity above ground has been observed only rarely in the native habitat [51]. Therefore, we tested the hypothesis that captive naked mole-rats would display a physiological sensitivity to the warmer, low CO_2 surface environment. Adult naked mole-rats were exposed to simulated nest conditions (2.5% CO_2/21% O_2/76.5% N_2 at 32°C), to room air (0.04% CO_2/21% O_2/78.96% N_2 at 20°C), or to simulated surface conditions [8], where room air was heated to 42°C. Respiratory rate measured under these environmental conditions demonstrated a significant effect of temperature, more than doubling during exposure to the simulated surface environment (Figure 2A). Systemic pH and blood CO_2 partial pressure values in naked mole-rats ranged from respiratory acidosis in the simulated nest conditions to relative hypocapnic alkalosis when exposed to the hyperthermia-promoting simulated surface conditions (Figure 2B). Hyperventilation often followed a period of motor hyperactivity in the simulated surface environment. This activity typically subsided after around 10 min. In 9 out of 10 animals exposed to simulated surface environment, signs of seizure activity (head-bobbing, mouth automatisms, generalized convulsions; Video S2) appeared after the cessation of hyperactivity, on average 14.4 ± 1.2 min after the chamber ambient temperature reached 42°C. Rectal temperature, measured after removal from the chamber heated to 42°C, averaged 41.7°C ± 0.6°C (n = 10). Animals demonstrating these seizures were males and females from four different colonies ranging in age from 5 months to nearly 4 years; nearly all were well past the age of sexual maturity (6 months) and considered adults, despite the presence of a number of neotenous features [28, 52, 53].

Figure 2C shows a representative cortical electroencephalogram (EEG) recording of seizure activity during exposure to a simulated surface environment (0.04% CO_2/21% O_2/78.96% N_2 at 42°C). Seizures produced in the simulated surface environment were prevented when simulated nest air at 42°C (2.5% CO_2/21% O_2/76.5% N_2) was deployed in the environmental chamber (Figure 2D). Wavelet decomposition and line-length analysis used to automatically identify epileptiform activity [54] confirmed experimenter observation of seizures in all of the EEG-implanted animals exposed to simulated surface environment containing low (0.04%) ambient CO_2 (n = 3), and in none of the animals exposed to the similarly heated high (2.5%) ambient CO_2 environment (n = 3). When animals removed from simulated surface conditions were exposed to simulated nest air (2.5% CO_2/21% O_2/76.5% N_2) after the beginning of a seizure, high-frequency, high-amplitude cortical seizure events subsided in the EEG (Figures 2C and 2D), but head-bobbing and mouth automatisms continued for the remainder of the experiment (>10 min).

The elevated respiratory rates and blood pH measured in naked mole-rats in the simulated surface environment (Figures 2A and 2B) indicate that respiratory alkalosis is the underlying seizure trigger, similar to seizures observed under similar conditions in children [55] and in rat and mouse pups [56–60]. In mice and rats, this high susceptibility to brain alkalosis-induced seizures subsides toward the third week of life [56], which in these species is closely paralleled by the developmental up-regulation of KCC2 and consequent maturation of GABAergic signaling [37, 61].

In humans, KCC2 is encoded by the solute carrier family 12 member 5 (*SLC12A5*) gene. Recently, an arginine to histidine mutation at site 952 of human KCC2b (KCC2-R952H; aka KCC2-R975H in the KCC2a splice variant), located in the highly conserved regulatory region encoded by exon 22, was identified by us as a loss-of-function mutation associated with febrile seizures in humans [41]. Examination of the published naked mole-rat genome [62, 63] revealed a histidine, uniquely among

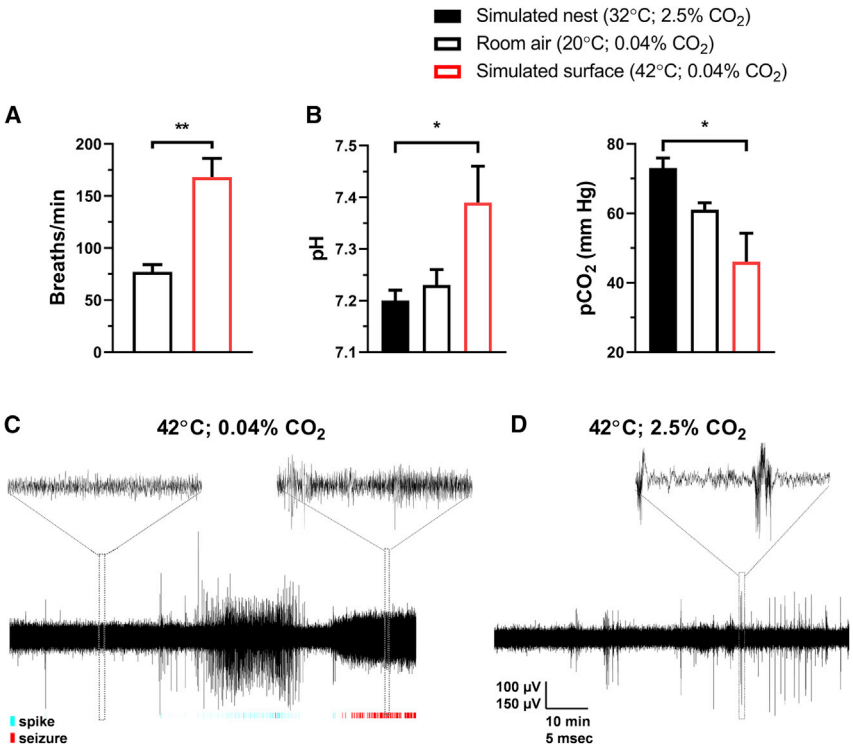

Figure 2. Hyperthermia-Induced Respiratory Alkalosis Promotes Seizures in Adult Naked Mole-Rats

(A) Hyperthermia increases breathing rate of naked mole-rats (n = 5). **p < 0.01, Mann-Whitney U test.

(B) Hyperthermia promotes systemic hypocapnic alkalosis in the naked mole-rat. Blood pH values range from acidosis in the simulated nest conditions (n = 3) and in room air (n = 4) to hypocapnic alkalosis in simulated surface conditions (n = 7) mimicking the warm aboveground conditions of the animal's native habitat in the Horn of Africa. pCO_2, partial pressure of CO_2. *p < 0.05, Kruskal-Wallis test, followed by Dunn's post hoc test.

(C and D) Cortical EEG recordings of naked mole-rats exposed to a chamber heated to 42°C containing (C) room air (0.04% CO_2) or (D) high CO_2-containing air (2.5% CO_2). Cyan and red marks indicate periods of abnormal spikes and seizures (respectively) detected by an automated line-length analysis based on the artifact-removed and wavelet-decomposed EEG trace [54]. Note the lack of abnormal spikes or seizures (cyan or red marks) detected in the presence of 2.5% ambient CO_2 (D). See Video S2 for an example of hyperthermia-induced seizure behavior.

mammals, as a species-specific variant at this homologous position in the orthologous gene encoding for KCC2 in the naked mole-rat (Figure 3). Intriguingly, we identified a cysteine variation in this position in the published genome [64] of the Damaraland mole-rat (*Fukomys damarensis*) (Figure 3), a close relative of the naked mole-rat and the only other eusocial mammal species noted to date. Both naked mole-rats and Damaraland mole-rats have been reported to lack clear behavioral responsiveness to high ambient CO_2 [22] (but see [65]). Naked mole-rats and Damaraland mole-rats are the only mammalian species with a native variant in this position in region encoded by exon 22 of KCC2. Figure S2 expands the analysis based on genomes of the euarchontoglires (supramammals) clade (Figure 3) to all published whole genomes across Mammalia to demonstrate the high conservation of this amino acid locus.

The species-specific point variant of KCC2 identified in naked mole-rats may have important consequences for neuronal physiology. Overexpression studies of human KCC2-H952 in mouse hippocampal and neocortical neurons have demonstrated that a histidine at this position reduces the expression of KCC2 in the neuronal plasma membrane, resulting in a lowered Cl^- extrusion capacity of neurons expressing KCC2-H952 compared to those expressing wild-type human KCC2 (KCC2-R952) [41, 43] (see also [66]).

To investigate the Cl^- extrusion capacity of cortical pyramidal neurons of 12-month-old naked mole-rats and 2-week-old mice, we performed patch clamp recordings of the reversal potential of $GABA_A$R-mediated currents (E_{GABA}), which reflects the level of intracellular Cl^- concentration. Upon somatically loading the neurons through the patch pipette with a defined constant Cl^- load of exactly the same magnitude, dendritic E_{GABA} values were determined by local puff application of GABA to a dendritic segment at a fixed (~50 µm) distance from the somatic Cl^- loading site. These experiments, performed under pharmacological block of bumetanide-sensitive secondary-active Cl^- uptake mechanisms [42], showed that, while the resting membrane potential of layer 2/3 pyramidal neurons were comparatively negative in, both, mice (n = 10) and naked mole-rats (n = 9), dendritic E_{GABA} values in the latter species were more positive, suggesting less efficient Cl^- extrusion under the present conditions (Figure 4A). Repetitive stimulation of GABAergic inputs on pyramidal neurons, particularly in the absence of efficient Cl^- extrusion, reduces the amplitude of these inputs due to activity-dependent accumulation of intraneuronal Cl^- and may even result in a change in polarity of $GABA_A$R-mediated currents [67, 68]. This situation is particularly relevant to neuronal compartments with high surface-to-volume ratio, such as dendrites, which are highly prone to fast activity-dependent shifts in E_{GABA} [37]. Notably, hyperthermic seizures triggered in immature animals by respiratory alkalosis may, under certain conditions, even be exacerbated by $GABA_A$R potentiation [59].

In light of the above, we set out to test whether a standard GABA-potentiating anticonvulsant, diazepam, would block hyperthermia-induced seizures in full-grown naked mole-rats. Strikingly, diazepam injected intraperitoneally not only failed to prevent seizures, but in fact *triggered* seizures when injected in room air at room temperature (20°C). Injection of 1 or 5 mg/kg diazepam (i.p.) in male and female adult naked mole-rats (weighing between 25 and 57 g and administered under ambient temperatures of 20°C or 32°C) produced motor convulsions in 10 out of 10 animals. The time to convulsions was typically less than 5 min following injection of 5 mg/kg diazepam (n = 5) and greater than 20 min following 1 mg/kg diazepam (n = 5). Two animals at each dose were implanted with EEG electrodes, and motor convulsion

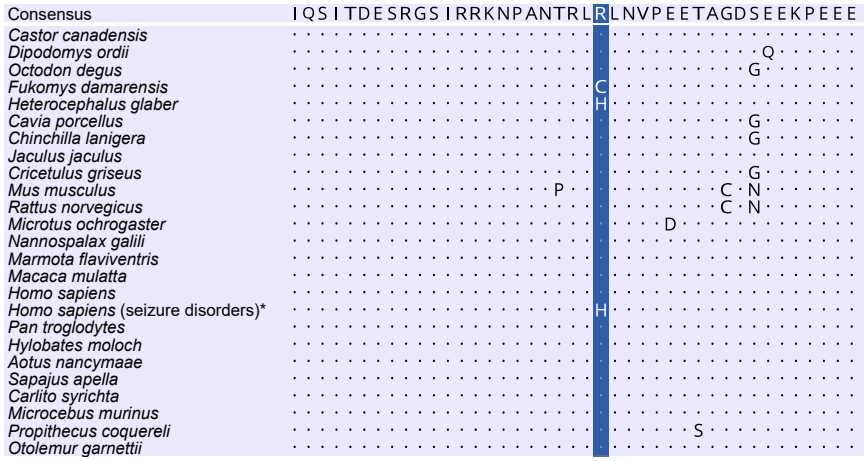

Figure 3. *In Silico* Analysis of the Naked Mole-Rat Genome Reveals a Species-Specific KCC2 Variant

Alignment of the amino acid sequences encoded by exon 22 of KCC2 orthologs in rodent and primate members of the euarchontoglires (supraprimates) clade. Figure S2 demonstrates how highly conserved this region is in all clades across Mammalia. Amino acid arginine (R) at position 952 (in human KCC2b; NCBI: NP_065759.1) is highly conserved among mammals with the exception of the two eusocial species, the naked mole-rat (*Heterocephalus glaber*; NCBI: XP_004858176.1), which carries a histidine (H), and the Damaraland mole-rat (*Fukomys damarensis*; NCBI: XP_010624588.1), which carries a cysteine (C) at this locus (based on the published genomes [62–64]). *The first human disease-related mutation of the gene encoding KCC2, an R-to-H mutation (R952H) at this same position, has been found in an Australian family with febrile seizures [41] and in a cohort of Canadian patients with idiopathic generalized epilepsy [43]. R952H has also been reported in human autism spectrum disorders and schizophrenia [44]. Analysis and alignment were done in Geneious Prime using NCBI protein sequences of mammalian KCC2/*SLC12A5* orthologs. Dots indicate adherence to the consensus sequence.

activity was confirmed to be accompanied by cortical seizures (Figure 4B). Administration of 0.5 mg/kg diazepam produced no sedation or behavioral signs of seizure in four of five animals injected; instead, increased (agitated) behavior was observed. The fifth animal injected with this this dose showed sedation for 20 min following injection. Thus, typically anticonvulsant doses of diazepam [59] elicit seizures in adult naked mole-rats, indicating an excitatory response to GABA *in vivo*.

In vitro extracellular electrophysiological recordings in hippocampal slices provide support that $GABA_AR$ can contribute to neuronal hyperexcitability in the adult naked mole-rat (Figure 4C). Slices of adult naked mole-rat hippocampus routinely showed unprovoked epileptiform burst discharges, similar to those measured in chronic rodent models of epilepsy [69], in the CA3 pyramidal cell layer under normal recording conditions. When the $GABA_AR$ agonist isoguvacine (200 μM) was added to the perfusate, slices that were bursting increased their bursting activity and developed spreading depression (n = 3 slices from 3 animals), indicating an excitatory response to $GABA_AR$ activation (Figure 4C).

DISCUSSION

Converging evidence from the current study posits CO_2 as an important and necessary environmental factor for naked mole-rat brain physiology. In a semi-natural laboratory colony housing environment, naked mole-rats establish clear nest areas that harbor elevated CO_2 levels. Analysis of the individual activity patterns of colony members demonstrates that all colony members spend the majority of their time in this part of the housing environment, regardless of caste or time of day. When exogenous CO_2 was applied to the colony environment outside of the nest, colony members made more visits to this CO_2-rich area and relocated the colony nest to the site of gas infusion, after the gas was turned off.

The most accurate estimates of naked mole-rat burrow air composition to date [16] show only mildly elevated ambient CO_2 levels in unoccupied or low occupied areas, within the range of what most mammals experience and can tolerate. However, the location of the colony nest at the deeper areas of the burrow, which have temperatures below the range of thermoneutrality for naked mole-rats (31°C–34°C) [8], suggests that huddling is a necessary form of thermoregulation [9]. In captivity, in an environment (29.2°C ± 1.4°C) maintained closer to their thermoneutral range, naked mole-rats exhibited consistent huddling behavior, which substantially increased ambient CO_2 in the nest chamber. When naked mole-rats were presently removed from the colony and exposed to hyperthermia (42°C), which was lower than the average temperature recorded at the surface of naked mole-rat burrows in Ethiopia (46.8°C [16]), the animals had seizures preceded by hyperventilation and the consequent systemic hypocapnic alkalosis [56]. Indeed, blood measures under these conditions showed a 36% reduction in CO_2 and a pH raised by 0.2 units.

Our analysis of the published naked mole-rat genomes [62, 63] revealed a species-specific loss-of-function histidine point variant in exon 22 of the gene encoding KCC2, a developmentally regulated cation-chloride cotransporter that is important for establishing the neuronal Cl^- gradient and thus the hyperpolarizing action of GABA [37]. The previous findings of this histidine variant in the gene encoding KCC2 in humans with febrile seizures [41] and epilepsy [43] indicate that this KCC2 variant is likely to promote hyperexcitability via decreased neuronal Cl^- extrusion. Here, we show attenuated Cl^- extrusion capacity in cortical neurons of the adult naked mole-rat, which is consistent with work demonstrating loss-of-function properties associated with this amino acid variation in human KCC2 [41, 43].

In line with our genomic and patch clamp data, moderate doses of diazepam, a GAB_AAR positive allosteric modulator, triggered EEG-confirmed seizures in normal air at room temperature. To our knowledge, the present study is the first to show that potentiating $GABA_ARs$ can elicit seizures *in vivo* in a mature mammal. The effect of diazepam was reversed when naked mole-rats were injected with the drug in a hypercapnia-inducing environment, where diazepam elicited

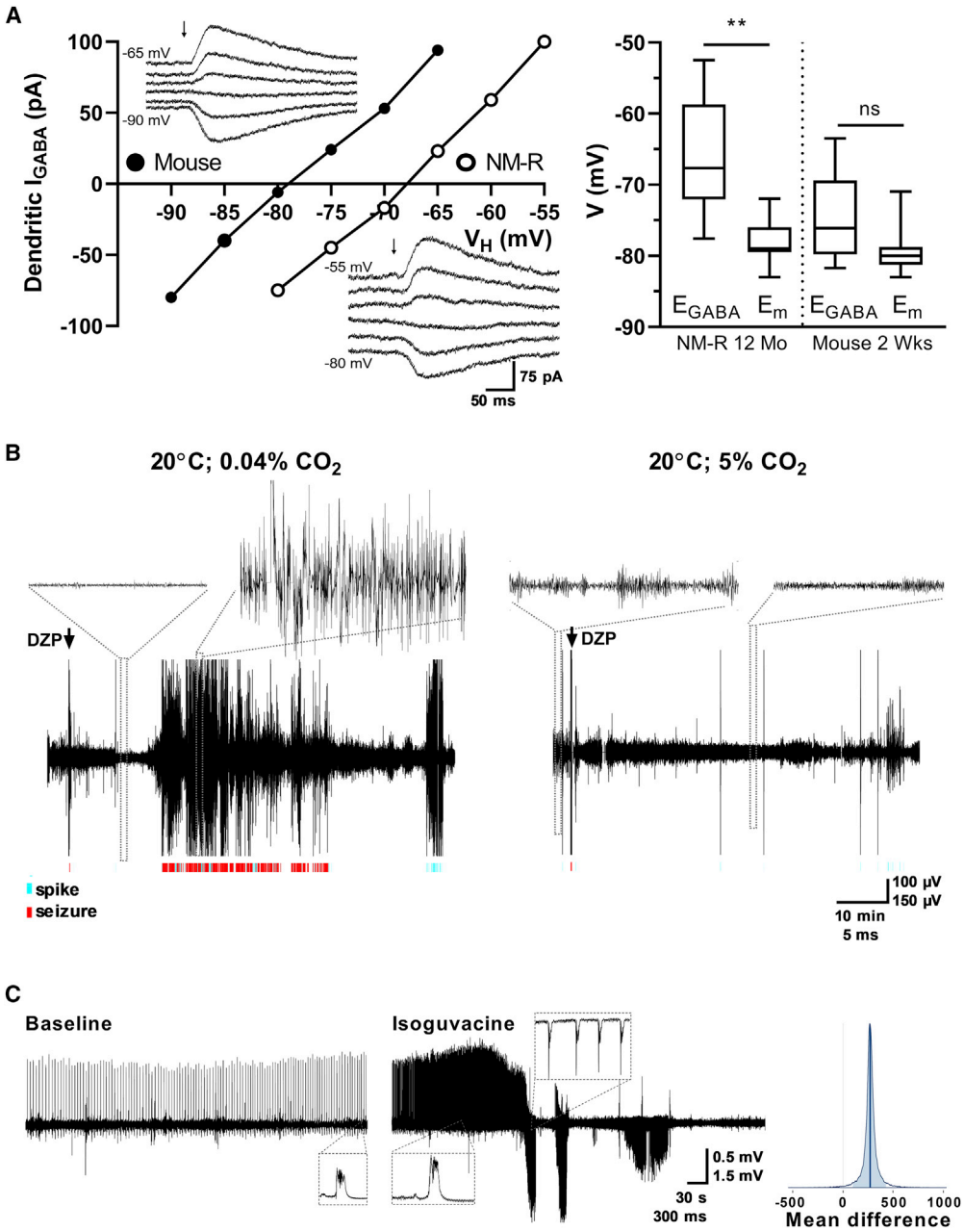

Figure 4. Reduced Neuronal Cl^- Extrusion and Excitatory Network Responses to $GABA_A$ Receptor Activation in the Adult Naked Mole-Rat

(A) Cl^- extrusion efficacy of neocortical pyramidal neurons in 12-month-old naked mole-rats and 2-week-old mice. Left: sample recordings of GABA-induced currents (I_{GABA}) evoked at a dendritic location 50 µm away from the somatic Cl^- loading site. Arrow indicates timing GABA pressure microinjection. Right: box-and-whisker (min-max range) plot of the reversal potential of dendritic $GABA_A$ receptor-mediated current (E_{GABA}) and resting membrane potential (E_m) illustrate a more depolarized E_{GABA} in the naked mole-rat (NM-R). **$p < 0.01$, Kruskal-Wallis test, followed by Dunn's post hoc test.

(B) EEG recordings during injection of diazepam (DZP). Left: animal at room temperature was injected i.p. with 1 mg/kg DZP. Colored lines indicate detected spike (cyan) and seizure (red) activity using a line-length analysis on the wavelet-decomposed signal. Right: presence of 5% CO_2 in the inhaled air prior to injection of DZP (1 mg/kg) prevented seizure occurrence.

(C) Hippocampal slice extracellular recordings from the CA3 pyramidal cell layer. Left: baseline recording under standard conditions exhibited epileptiform bursting. Middle: $GABA_AR$ agonist isoguvacine (200 µM) administered in the bath solution induced high-frequency bursting followed by spreading depression. Right: posterior distribution of burst power mean difference showing the 95% highest density interval, which does not cross zero, demonstrating a significant increase in burst power by isoguvacine.

a typical sedative response. In a hypercapnia-adapted species, such as the naked mole-rat, the low atmospheric levels of CO_2 are likely to increase network activity and thus promote activity-dependent Cl^- loading of post-synaptic neurons at GABAergic synapses [37]. Our data indicate that naked mole-rat cortical neurons possess a relatively low capacity for extrusion of intraneuronal Cl^-, and the consequent low level of inhibitory GABAergic tone under conditions of normal atmospheric CO_2 levels is counteracted by the anticonvulsant properties of hypercapnia in the nest.

We propose that the anticonvulsant action of elevated CO_2 in the naked mole-rat colony nest has acted as a selection pressure for mutations that conserve energy at the expense of GABAergic inhibition [30, 36] in a hypoxic environment. Support for this comes from our observation that the Damaraland mole-rat, the only other eusocial mammal identified to date, is the only other mammal with a non-consensus amino acid at the pertinent locus in the exon 22 of KCC2. Our findings may therefore shed light on a proximate cause for the extremely low rates of dispersal in eusocial mammals.

STAR★METHODS

Detailed methods are provided in the online version of this paper and include the following:

- KEY RESOURCES TABLE
- LEAD CONTACT AND MATERIALS AVAILABILITY
- EXPERIMENTAL MODEL AND SUBJECT DETAILS
- METHOD DETAILS
  - Colony behavior observations
  - Quantitative analysis of congregation
  - Colony CO_2 measurements
  - Exogenous CO_2 delivery to colony
  - Surgery and EEG Recording
  - Induction of hyperthermic seizures
  - Patch clamp recordings from cortical pyramidal neurons
  - Extracellular field recordings from hippocampal slices
- QUANTIFICATION AND STATISTICAL ANALYSIS
- DATA AND CODE AVAILABILITY

SUPPLEMENTAL INFORMATION

Supplemental Information can be found online at https://doi.org/10.1016/j.cub.2020.03.071.

ACKNOWLEDGMENTS

This work was supported by a NSF CAREER Award 1149446 (to D.P.M.) and by the Emil Aaltonen Foundation (grants 160220 N1V and 180206 N1V to M.P.), by the Academy of Finland (grants 319237 and 294375 to K.K.), and by the Jane and Aatos Erkko Foundation (to K.K.). Computational support was provided by The City University of New York High Performance Computing Center, which is operated by the College of Staten Island, funded, in part, by The City University of New York, the Research Foundation of CUNY, and grants from the National Science Foundation CNS-0958379 and CNS-0855217. We thank Bruce Goldman for original animal stock and training, and Margherita Sansone and the College of Staten Island Animal Care staff for assistance. This paper is dedicated to the memory of our coauthor Edward F. Meehan.

AUTHOR CONTRIBUTIONS

Conceptualization, M.Z., K.K., M.P., and D.P.M.; Study Design, M.Z., E.F.M., M.E.K., K.K., M.P., and D.P.M.; Methodology, M.Z., E.F.M., M.E.K., D.T., M.P., and D.P.M.; Investigation, M.Z., E.F.M., M.E.K., D.T., M.P., and D.P.M.; Writing – Original Draft, M.Z., M.P., and D.P.M.; Writing – Review and Editing, M.Z., E.F.M., K.K., M.P., and D.P.M.; Funding Acquisition, M.E.K., K.K., M.P., and D.P.M.

DECLARATION OF INTERESTS

The authors declare no competing interests.

Received: January 22, 2019
Revised: November 27, 2019
Accepted: March 30, 2020
Published: April 30, 2020

REFERENCES

1. Jarvis, J.U.M., and Bennett, N.C. (1993). Eusociality has evolved independently in two genera of bathyergid mole-rats — but occurs in no other subterranean mammal. Behav. Ecol. Sociobiol. *33*, 253–260.
2. Alexander, R.D., Noonan, K.M., and Crespi, B.J. (1991). The evolution of eusociality. In The Biology of the Naked Mole-Rat, P.W. Sherman, J.U.M. Jarvis, and R.D. Alexander, eds. (Princeton University Press), pp. 3–44.
3. Faulkes, C.G., and Bennett, N.C. (2013). Plasticity and constraints on social evolution in African mole-rats: ultimate and proximate factors. Philos. Trans. R. Soc. Lond. B Biol. Sci. *368*, 20120347.
4. Jarvis, J.U. (1981). Eusociality in a mammal: cooperative breeding in naked mole-rat colonies. Science *212*, 571–573.
5. Nowak, M.A., Tarnita, C.E., and Wilson, E.O. (2010). The evolution of eusociality. Nature *466*, 1057–1062.
6. Brett, R.A. (1991). The ecology of naked mole-rat colonies. In The Biology of the Naked Mole-Rat, P. Sherman, J.U.M. Jarvis, and R. Alexander, eds. (Princeton University Press), pp. 137–184.
7. Judd, T.M., and Sherman, P.W. (1996). Naked mole-rats recruit colony mates to food sources. Anim. Behav. *52*, 957–969.
8. Buffenstein, R., and Yahav, S. (1991). Is the naked mole-rat Hererocephalus glaber an endothermic yet poikilothermic mammal? J. Therm. Biol. *16*, 227–232.
9. Yahav, S., and Buffenstein, R. (1991). Huddling behavior facilitates homeothermy in the naked mole rat Heterocephalus glaber. Physiol. Zool. *64*, 871–884.
10. Goldman, B.D., Goldman, S.L., Lanz, T., Magaurin, A., and Maurice, A. (1999). Factors influencing metabolic rate in naked mole-rats (Heterocephalus glaber). Physiol. Behav. *66*, 447–459.
11. Buffenstein, R. (2005). The naked mole-rat: a new long-living model for human aging research. J. Gerontol. A Biol. Sci. Med. Sci. *60*, 1369–1377.
12. Buffenstein, R. (2009). Ecophysiological responses to a subterranean habitat; a Bathyergid perspective. Mammalia *60*, 591–606.
13. Johansen, K., Lykkeboe, G., Weber, R.E., and Maloiy, G.M.O. (1976). Blood respiratory properties in the naked mole rat Heterocephalus glaber, a mammal of low body temperature. Respir. Physiol. *28*, 303–314.
14. Larson, J., Drew, K.L., Folkow, L.P., Milton, S.L., and Park, T.J. (2014). No oxygen? No problem! Intrinsic brain tolerance to hypoxia in vertebrates. J. Exp. Biol. *217*, 1024–1039.
15. Park, T.J., Reznick, J., Peterson, B.L., Blass, G., Omerbašić, D., Bennett, N.C., Kuich, P.H.J.L., Zasada, C., Browe, B.M., Hamann, W., et al. (2017). Fructose-driven glycolysis supports anoxia resistance in the naked mole-rat. Science *356*, 307–311.
16. Holtze, S., Braude, S., Lemma, A., Koch, R., Morhart, M., Szafranski, K., Platzer, M., Alemayehu, F., Goeritz, F., and Hildebrandt, T.B. (2018). The

microenvironment of naked mole-rat burrows in East Africa. Afr. J. Ecol. *56*, 279–289.

17. Bennett, N.C., Jarvis, J.U.M., and Davies, K.C. (1988). Daily and seasonal temperatures in the burrows of African rodent moles. Afr. Zool. *23*, 189–195.
18. Chung, D., Dzal, Y.A., Seow, A., Milsom, W.K., and Pamenter, M.E. (2016). Naked mole rats exhibit metabolic but not ventilatory plasticity following chronic sustained hypoxia. Proc. Biol. Sci. *283*, 20160216.
19. Clayson, M.S., Devereaux, M.E.M., and Pamenter, M.E. (2020). Neurokinin-1 receptor activation is sufficient to restore the hypercapnic ventilatory response in the Substance P-deficient naked mole-rat. Am. J. Physiol. Regul. Integr. Comp. Physiol. *318*, R712–R721.
20. Roper, T.J., Bennett, N.C., Conradt, L., and Molteno, A.J. (2001). Environmental conditions in burrows of two species of African mole-rat, Georhychus capensis and Cryptomys damarensis. J. Zool. (Lond.) *254*, 101–107.
21. Nathaniel, T.I., Otukonyong, E., Abdellatif, A., and Soyinka, J.O. (2012). Effect of hypoxia on metabolic rate, core body temperature, and c-fos expression in the naked mole rat. Int. J. Dev. Neurosci. *30*, 539–544.
22. Branigan, T., Elkhalifa, S., and Pamenter, M.E. (2018). Behavioural responses to environmental hypercapnia in two eusocial species of African mole rats. J. Comp. Physiol. A Neuroethol. Sens. Neural Behav. Physiol. *204*, 811–819.
23. Kirby, A.M., Fairman, G.D., and Pamenter, M.E. (2018). Atypical behavioural, metabolic and thermoregulatory responses to hypoxia in the naked mole rat (*Heterocephalus glaber*). J. Zool. (Lond.) *305*, 106–115.
24. de Wolf, E., Cook, J., and Dale, N. (2017). Evolutionary adaptation of the sensitivity of connexin26 hemichannels to CO2. Proc. Biol. Sci. *284*, 20162723.
25. Park, T.J., Lu, Y., Jüttner, R., Smith, E.S.J., Hu, J., Brand, A., Wetzel, C., Milenkovic, N., Erdmann, B., Heppenstall, P.A., et al. (2008). Selective inflammatory pain insensitivity in the African naked mole-rat (Heterocephalus glaber). PLoS Biol. *6*, e13.
26. Smith, E.S.J., Omerbašić, D., Lechner, S.G., Anirudhan, G., Lapatsina, L., and Lewin, G.R. (2011). The molecular basis of acid insensitivity in the African naked mole-rat. Science *334*, 1557–1560.
27. Husson, Z., and Smith, E.S.J. (2018). Naked mole-rat cortical neurons are resistant to acid-induced cell death. Mol. Brain *11*, 26.
28. Orr, M.E., Garbarino, V.R., Salinas, A., and Buffenstein, R. (2016). Extended postnatal brain development in the longest-lived rodent: prolonged maintenance of neotenous traits in the naked mole-rat brain. Front. Neurosci. *10*, 504.
29. Herculano-Houzel, S., Ribeiro, P., Campos, L., Valotta da Silva, A., Torres, L.B., Catania, K.C., and Kaas, J.H. (2011). Updated neuronal scaling rules for the brains of Glires (rodents/lagomorphs). Brain Behav. Evol. *78*, 302–314.
30. Buzsáki, G., Kaila, K., and Raichle, M. (2007). Inhibition and brain work. Neuron *56*, 771–783.
31. Lee, J., Taira, T., Pihlaja, P., Ransom, B.R., and Kaila, K. (1996). Effects of CO_2 on excitatory transmission apparently caused by changes in intracellular pH in the rat hippocampal slice. Brain Research *706*, 210–216.
32. Zappe, A.C., Uludağ, K., Oeltermann, A., Uğurbil, K., and Logothetis, N.K. (2008). The influence of moderate hypercapnia on neural activity in the anesthetized nonhuman primate. Cereb. Cortex *18*, 2666–2673.
33. Xu, F., Uh, J., Brier, M.R., Hart, J., Jr., Yezhuvath, U.S., Gu, H., Yang, Y., and Lu, H. (2011). The influence of carbon dioxide on brain activity and metabolism in conscious humans. J. Cereb. Blood Flow Metab. *31*, 58–67.
34. Woodbury, D.M., Rollins, L.T., Gardner, M.D., Hirschi, W.L., Hogan, J.R., Rallison, M.L., Tanner, G.S., and Brodie, D.A. (1958). Effects of carbon dioxide on brain excitability and electrolytes. Am. J. Physiol. *192*, 79–90.
35. Tolner, E.A., Hochman, D.W., Hassinen, P., Otáhal, J., Gaily, E., Haglund, M.M., Kubová, H., Schuchmann, S., Vanhatalo, S., and Kaila, K. (2011). Five percent CO_2 is a potent, fast-acting inhalation anticonvulsant. Epilepsia *52*, 104–114.
36. Kaila, K., Ruusuvuori, E., Seja, P., Voipio, J., and Puskarjov, M. (2014). GABA actions and ionic plasticity in epilepsy. Curr. Opin. Neurobiol. *26*, 34–41.
37. Kaila, K., Price, T.J., Payne, J.A., Puskarjov, M., and Voipio, J. (2014). Cation-chloride cotransporters in neuronal development, plasticity and disease. Nat. Rev. Neurosci. *15*, 637–654.
38. Pond, B.B., Galeffi, F., Ahrens, R., and Schwartz-Bloom, R.D. (2004). Chloride transport inhibitors influence recovery from oxygen-glucose deprivation-induced cellular injury in adult hippocampus. Neuropharmacology *47*, 253–262.
39. Tao, R., Li, C., Newburn, E.N., Ye, T., Lipska, B.K., Herman, M.M., Weinberger, D.R., Kleinman, J.E., and Hyde, T.M. (2012). Transcript-specific associations of SLC12A5 (KCC2) in human prefrontal cortex with development, schizophrenia, and affective disorders. J. Neurosci. *32*, 5216–5222.
40. Ben-Ari, Y., Khalilov, I., Kahle, K.T., and Cherubini, E. (2012). The GABA excitatory/inhibitory shift in brain maturation and neurological disorders. Neuroscientist *18*, 467–486.
41. Puskarjov, M., Seja, P., Heron, S.E., Williams, T.C., Ahmad, F., Iona, X., Oliver, K.L., Grinton, B.E., Vutskits, L., Scheffer, I.E., et al. (2014). A variant of KCC2 from patients with febrile seizures impairs neuronal Cl- extrusion and dendritic spine formation. EMBO Rep. *15*, 723–729.
42. Puskarjov, M., Kahle, K.T., Ruusuvuori, E., and Kaila, K. (2014). Pharmacotherapeutic targeting of cation-chloride cotransporters in neonatal seizures. Epilepsia *55*, 806–818.
43. Kahle, K.T., Merner, N.D., Friedel, P., Silayeva, L., Liang, B., Khanna, A., Shang, Y., Lachance-Touchette, P., Bourassa, C., Levert, A., et al. (2014). Genetically encoded impairment of neuronal KCC2 cotransporter function in human idiopathic generalized epilepsy. EMBO Rep. *15*, 766–774.
44. Merner, N.D., Chandler, M.R., Bourassa, C., Liang, B., Khanna, A.R., Dion, P., Rouleau, G.A., and Kahle, K.T. (2015). Regulatory domain or CpG site variation in SLC12A5, encoding the chloride transporter KCC2, in human autism and schizophrenia. Front. Cell. Neurosci. *9*, 386.
45. Stödberg, T., McTague, A., Ruiz, A.J., Hirata, H., Zhen, J., Long, P., Farabella, I., Meyer, E., Kawahara, A., Vassallo, G., et al. (2015). Mutations in SLC12A5 in epilepsy of infancy with migrating focal seizures. Nat. Commun. *6*, 8038.
46. Saitsu, H., Watanabe, M., Akita, T., Ohba, C., Sugai, K., Ong, W.P., Shiraishi, H., Yuasa, S., Matsumoto, H., Beng, K.T., et al. (2016). Impaired neuronal KCC2 function by biallelic SLC12A5 mutations in migrating focal seizures and severe developmental delay. Sci. Rep. *6*, 30072.
47. Payne, J.A., Stevenson, T.J., and Donaldson, L.F. (1996). Molecular characterization of a putative K-Cl cotransporter in rat brain. A neuronal-specific isoform. J. Biol. Chem. *271*, 16245–16252.
48. Antrobus, S.P., Lytle, C., and Payne, J.A. (2012). K+-Cl- cotransporter-2 KCC2 in chicken cardiomyocytes. Am. J. Physiol. Cell Physiol. *303*, C1180–C1191.
49. McCloskey, D.P., Kress, M.E., Imberman, S.P., Kushnir, I., and Briffa-Mirabella, S. (2011). From market baskets to mole rats: Using data mining techniques to analyze RFID data describing laboratory animal behavior. Proceedings of the 17th ACM SIGKDD International Conference on Knowledge Discovery and Data Mining, 301–306.
50. Alberts, J.R. (2007). Huddling by rat pups: ontogeny of individual and group behavior. Dev. Psychobiol. *49*, 22–32.
51. Braude, S. (2000). Dispersal and new colony formation in wild naked mole-rats: evidence against inbreeding as the system of mating. Behav. Ecol. *11*, 7–12.
52. Penz, O.K., Fuzik, J., Kurek, A.B., Romanov, R., Larson, J., Park, T.J., Harkany, T., and Keimpema, E. (2015). Protracted brain development in a rodent model of extreme longevity. Sci. Rep. *5*, 11592.
53. Skulachev, V.P., Holtze, S., Vyssokikh, M.Y., Bakeeva, L.E., Skulachev, M.V., Markov, A.V., Hildebrandt, T.B., and Sadovnichii, V.A. (2017).

Neoteny, prolongation of youth: From naked mole rats to ”naked apes” (humans). Physiol. Rev. *97*, 699–720.

54. Bergstrom, R.A., Choi, J.H., Manduca, A., Shin, H.S., Worrell, G.A., and Howe, C.L. (2013). Automated identification of multiple seizure-related and interictal epileptiform event types in the EEG of mice. Sci. Rep. *3*, 1483.
55. Schuchmann, S., Hauck, S., Henning, S., Grüters-Kieslich, A., Vanhatalo, S., Schmitz, D., et al. (2011). Respiratory alkalosis in children with febrile seizures. Epilepsia *52*, 1949–1955.
56. Schuchmann, S., Schmitz, D., Rivera, C., Vanhatalo, S., Salmen, B., Mackie, K., Sipilä, S.T., Voipio, J., and Kaila, K. (2006). Experimental febrile seizures are precipitated by a hyperthermia-induced respiratory alkalosis. Nat. Med. *12*, 817–823.
57. Schuchmann, S., Tolner, E.A., Marshall, P., Vanhatalo, S., and Kaila, K. (2008). Pronounced increase in breathing rate in the “hair dryer model” of experimental febrile seizures. Epilepsia *49*, 926–928.
58. Ruusuvuori, E., and Kaila, K. (2014). Carbonic anhydrases and brain pH in the control of neuronal excitability. Subcell. Biochem. *75*, 271–290.
59. Ruusuvuori, E., Huebner, A.K., Kirilkin, I., Yukin, A.Y., Blaesse, P., Helmy, M., Kang, H.J., El Muayed, M., Hennings, J.C., Voipio, J., et al. (2013). Neuronal carbonic anhydrase VII provides GABAergic excitatory drive to exacerbate febrile seizures. EMBO J. *32*, 2275–2286.
60. Pospelov, A.S., Yukin, A.Y., Blumberg, M.S., Puskarjov, M., and Kaila, K. (2016). Forebrain-independent generation of hyperthermic convulsions in infant rats. Epilepsia *57*, e1–e6.
61. Rivera, C., Voipio, J., and Kaila, K. (2005). Two developmental switches in GABAergic signalling: the K+-Cl- cotransporter KCC2 and carbonic anhydrase CAVII. J. Physiol. *562*, 27–36.
62. Kim, E.B., Fang, X., Fushan, A.A., Huang, Z., Lobanov, A.V., Han, L., Marino, S.M., Sun, X., Turanov, A.A., Yang, P., et al. (2011). Genome sequencing reveals insights into physiology and longevity of the naked mole rat. Nature *479*, 223–227.
63. Keane, M., Craig, T., Alföldi, J., Berlin, A.M., Johnson, J., Seluanov, A., Gorbunova, V., Di Palma, F., Lindblad-Toh, K., Church, G.M., and de Magalhães, J.P. (2014). The Naked Mole Rat Genome Resource: facilitating analyses of cancer and longevity-related adaptations. Bioinformatics *30*, 3558–3560.
64. Fang, X., Seim, I., Huang, Z., Gerashchenko, M.V., Xiong, Z., Turanov, A.A., Zhu, Y., Lobanov, A.V., Fan, D., Yim, S.H., et al. (2014). Adaptations to a subterranean environment and longevity revealed by the analysis of mole rat genomes. Cell Rep. *8*, 1354–1364.
65. Zhang, S.Y., and Pamenter, M.E. (2019). Fossorial Damaraland mole rats do not exhibit a blunted hypercapnic ventilatory response. Biol. Lett. *15*. 20190006. https://doi.org/10.1098/rsbl.2019.0006.
66. Mavrovic, M., Uvarov, P., Delpire, E., Vutskits, L., Kaila, K., and Puskarjov, M. (2020). Loss of non-canonical KCC2 functions promotes developmental apoptosis of cortical projection neurons. EMBO Rep. *21*, e48880. https://doi.org/10.15252/embr.201948880.
67. Kaila, K., Lamsa, K., Smirnov, S., Taira, T., and Voipio, J. (1997). Long-lasting GABA-mediated depolarization evoked by high-frequency stimulation in pyramidal neurons of rat hippocampal slice is attributable to a network-driven, bicarbonate-dependent K+ transient. J. Neurosci. *17*, 7662–7672.
68. Taira, T., Lamsa, K., and Kaila, K. (1997). Posttetanic excitation mediated by GABA(A) receptors in rat CA1 pyramidal neurons. J. Neurophysiol. *77*, 2213–2218.
69. McCloskey, D.P., and Scharfman, H.E. (2011). Progressive, potassium-sensitive epileptiform activity in hippocampal area CA3 of pilocarpine-treated rats with recurrent seizures. Epilepsy Res. *97*, 92–102.
70. McCloskey, D.P., Croll, S.D., and Scharfman, H.E. (2005). Depression of synaptic transmission by vascular endothelial growth factor in adult rat hippocampus and evidence for increased efficacy after chronic seizures. J. Neurosci. *25*, 8889–8897.
71. Brodersen, K.H., Gallusser, F., Koehler, J., Remy, N., and Scott, S.L. (2015). Inferring causal impact using Bayesian structural time-series models. Ann. Appl. Stat. *9*, 247–274.
72. Puskarjov, M., Fiumelli, H., Briner, A., Bodogan, T., Demeter, K., Lacoh, C.M., et al. (2017). K-Cl cotransporter 2-mediated Cl- extrusion determines developmental stage-dependent Impact of propofol anesthesia on dendritic spines. Anesthesiology *126*, 855–867.

STAR★METHODS

KEY RESOURCES TABLE

REAGENT or RESOURCE	SOURCE	IDENTIFIER
Chemicals, Peptides, and Recombinant Proteins		
Diazepam	Henry Schein	Cat. No. 1278188
Isoflurane	Vet One	Cat. No. 501017
Ketoprofen	Zoetis	https://www.zoetisus.com/products/horses/ketofen.aspx
Bumetanide	Tocris	Cat. No.3108
TTX	Tocris	Cat. No. 1078
CGP 55845	Tocris	Cat. No. 1248
CNQX	Tocris	Cat. No. 1045
D-AP5	Tocris	Cat. No. 0106
GABA	Tocris	Cat. No. 0386
Isoguvacine	Tocris	Cat. No. 1298
Deposited Data		
African naked mole-rat colony behavior based on whole colony radio frequency identification (colony TT-2, April 2015)	This Paper	https://academicworks.cuny.edu/si_pubs/202
Carbon dioxide attracts nesting behavior in captive African naked mole-rats	This Paper	https://academicworks.cuny.edu/si_pubs/201
Software and Algorithms		
The R Project for Statistical Computing	The R Foundation	https://www.r-project.org/
Causal Impact Package in R	Developed by [70].	https://cran.r-project.org/web/packages/CausalImpact/CausalImpact.pdf
IgorR Package in R	Developed by G Jefferis	https://cran.r-project.org/web/packages/IgorR/IgorR.pdf
Pracma Package in R	Developed by HW Borchers	https://cran.r-project.org/web/package/pracma/pracma.pdf
IgorPro (6)	Wavemetrics	https://www.wavemetrics.com/
Geneious Prime	Biomatters	https://www.geneious.com
MATLAB (R2018b)	Mathworks	https://www.mathworks.com/
Trojan Unique RFID System	Dorset	https://www.dorset.nu/identification/rfid-products/
LabQuest Mini Sensor	Vernier	https://www.vernier.com/product/labquest-mini/
Sirenia Acquisition	Pinnacle Technologies	https://www.pinnaclet.com/software.html
Gem Premier 4000 Blood Gas Analyzer	Instrumentation Laboratory	https://www.instrumentationlaboratory.com
Patchmaster	HEKA Elektronic	https://www.heka.com/
Other		
Microcontrolled gas valve	Biospherix	https://www.biospherix.com/products/proox-c21

LEAD CONTACT AND MATERIALS AVAILABILITY

Further information and requests should be directed to and will be fulfilled by the Lead Contact, Dan McCloskey (dan.mccloskey@csi.cuny.edu). This study did not generate new unique reagents.

EXPERIMENTAL MODEL AND SUBJECT DETAILS

All methods involving animals were approved by the Institutional Animal Care and Use Committee at the College of Staten Island in the City University of New York and are in accordance with regulations required by the United States Department of Agriculture. Naked mole-rats (*Heterocephalus glaber*) were maintained in colonies bred from animals originally provided by Bruce Goldman

(UCONN). Five colonies of naked mole-rats (D-1, L-3, L-4, TT-1, TT-2) were housed in a 12h:12h low-light (50 Lux): dark (< 1 Lux) environment (lights on: 7AM) maintained in a temperature (29.2 ± 1.4°C) and relative humidity (20%) controlled room (5 x 7 m). Semi-naturalistic housing environments, established for each colony, were comprised of a series of 5 cm inner diameter clear polycarbonate tubes connecting square (27 × 32.5 × 10 cm) or rectangular (53 × 32.5 × 10 cm) chambers (polycarbonate steam table pans with solid lids). Reptile heat cables were used under the cages to provide additional warmth to segments of each cage. A few centimeters of corncob bedding, supplemented with pelleted rolled paper bedding, was placed in the bottom of each chamber. The size of the housing environment was determined by the size of the colony such that there is roughly one chamber for every 5-10 animals. Animals were fed *ad libitum* on a mixed diet of tubers, squash, fruits and Teklad Global 2019 lab chow (Harlan). The entire colony was disassembled and cleaned approximately every two weeks and individual toilet chambers were checked and cleaned daily on weekdays.

METHOD DETAILS

Colony behavior observations

Two colonies (L-4, n = 37; TT-2, n = 36) were arranged in semi-naturalistic environments equipped with twenty RFID antennas positioned between chambers to track the movements of each animal between chambers over extended periods of time. Each animal in the colony was implanted with a Trovan Unique (Dorset) RFID transponder (11.5 × 2.2 mm) injected under the skin. RFID antennas, circular in shape (100 mm inner-diameter), were placed around the tubing in the colony. When an animal passed an RFID antenna, a record of this action was entered into a text file by the Trovan software. Events recorded from each antenna were passed to a computer at a maximum rate of 10 events per second. Events were entered into a single text file, with each event containing the RFID tag number that was read, the antenna where the reading occurred, and the date and time of the reading. The feeding chamber of each colony was determined by the caregiver (the cage closest to the room entrance). Toilet chambers were determined by the colony and varied within each colony, but were always single entry (dead end) small chambers of the colony structure. Toilet chambers were easily identifiable as they were devoid of corncob bedding and were the only chambers that contained excrement. Certain chambers were identifiable as nest chambers, as they contained nearly all of the unrolled paper bedding, and often had a mass of animals huddled in them; these nest locations were determined by the colony members. A single nest chamber was typically observed for a colony, although as many as three nest chambers have been observed at times. A dataset for each colony was selected as a 25.58-day (614-h) series for L-4 (collected November 4-30, 2016), and a 26.67-day (640-h) series for TT-2 (collected April 1-27, 2015).The full dataset is available through CUNY Academic Works: https://academicworks.cuny.edu/si_pubs/202. Each collection period included four 60-h weekend periods (selected for minimal staff activity) for a second detailed analysis.

Quantitative analysis of congregation

The RFID data were preprocessed to correct misreads and eliminate duplicate reads created when animals loitered under an antenna. A state matrix, compiled in MATLAB using custom code, was populated by the last identified location for each animal and updated for every new entry in the RFID data file. Activity was measured by moves, which were defined as a reading at a different antenna location from the last known antenna, or at the same antenna location after the animal has moved away from the antenna range (which was approximately 4 cm). Although the antennas were positioned at the tunnels near entryways to chambers, our observation demonstrated that moves primarily represented activity between or within chambers, as prolonged stationary positioning in tunnels was rare. A stringent metric for stationary behavior was developed wherein not moving or remaining stationary was defined in units of an entire hour passing in which an individual animal was not read at a new antenna location. Proportion of time spent in the colony nest chambers (defined as the chamber with the highest density of animals in any given hour) and the colony food chamber (which is stable and determined by the animal care staff) was measured across each 60-h period. Proportion of time spent in the nest was measured for each colony member and averaged across each of the 600+ h epochs.

Colony CO_2 measurements

CO_2 levels were measured repeatedly in 96 chambers across all naked mole-rat colonies by siphoning chamber gas into a polycarbonate bottle using Tygon tubing and a handheld vacuum pump. The siphon tubing was carefully inserted to a corner of the chamber beneath the lid in order to avoid disturbing any animals in the chamber. Complete filling of the bottle was confirmed by displacement of water to a second bottle in sequence. CO_2 levels were recorded immediately after siphoning using a Vernier CO_2 sensor interfaced with a LabQuest Mini and a computer running Graphical Analysis software. These measures of air siphoned from the top of the chamber are likely an underestimate of the CO_2 levels encountered by animals at the chamber floor, especially inside of a huddle, but they are sufficient to examine the relationship between aggregation and chamber CO_2 levels.

Exogenous CO_2 delivery to colony

After a 24-h baseline period, 100% CO_2 was infused into non-nest chambers of the L-2 and TT-2 colonies through a microcontrolled gas valve (Biospherix) at a pressure < 5 psi. The valve closed as the CO_2 reached 11% (in the L-2 colony), or 2.5% (in the TT-2 colony). Following a recovery period, compressed air (colony L-2) or 100% N_2 (colony TT-2) was infused into the test chamber, with the gas valve set to close when the chamber CO_2 levels were below 0.01%. Analysis of the effects of gas infusion on animal behavior included both visits to the test chamber, measured by RFID events at antennas around the test chamber, and a USB video camera positioned

over the chamber, and computational analysis of nesting behavior in the colony TT-2 experiment. Average hourly events at the RFID antennas surrounding the test chamber were measured for each of the baseline and gas infusion period. The full RFID dataset of this experiment is availble for download at CUNY Academic Works: https://academicworks.cuny.edu/si_pubs/201. Statistical analysis of the effect of gas infusion on nesting behavior in the TT-2 experiment was achieved using a Bayesian structural time series model within the CausalImpact package in R [71]. The nesting location for each animal was computed for each hour over the 185-h experiment as the chamber with the predominant location for that animal during the hour. The model analyzed the proportion of animals in the test chamber (Chamber M) with activity for each hour at all of the RFID antennas around the TT-2 colony offered as predictor variables. The model was based on 1000 iterations of the time series data using a Gibbs sampling algorithm. The 95% highest density interval was used as a threshold for significance.

Surgery and EEG Recording

Male and female adult naked mole-rats weighing more than 35 g (over one year of age) were deeply anesthetized with isoflurane and placed in a mouse stereotaxic apparatus (Kopf) equipped with a nosecone to continue delivery of anesthesia at a concentration of 2.5%–3% and a flow rate of 0.5 LPM. Animals were maintained on a heating pad and monitored with a rectal thermometer for a target temperature of 30°C. Following confirmation of general anesthesia and cleaning and local anesthesia of the scalp with lidocaine, the skull surface was exposed via incision and a Pinnacle Technologies prefabricated three channel surface mount was secured to the skull with posterior screw electrodes drilled ± 2.5 mm ML and −1.27 mm AP from bregma. Anterior screws were aligned with the holes of the surface mount, and the headstage was secured in place with dental acrylic. Animals were allowed to recover for one week before recording, with post-surgical monitoring and ketoprofen (5 mg/kg, i.p.) treatment for three days. EEG recordings were made using Sirenia acquisition software (Pinnacle Technologies) and exported in European data format for subsequent processing in MATLAB. Movement artifact, detected as events in the EMG channel which exceeded two times the channel standard deviation and lasted for more than 250 ms, were set to zero within the EEG channels, and a fourth-order wavelet decomposition and line length analysis was applied to the cleaned EEG signal using previously developed MATLAB scripts [54]. Seizure events were considered events lasting more than five seconds and exceeding three times the standard deviation of the median line length of a 5-min baseline at the start of the recording. Automated event detection was tested against visual analysis by another researcher and matched with video of convulsions.

Induction of hyperthermic seizures

Male and female adult naked mole-rats (aged between five months and four years, 35-75 g) were introduced individually into a circular custom glove box chamber (35 × 22 cm) equipped with a video camera (GoPro Hero 4), a k-type thermocouple interfaced to a digital thermometer (Nicety), a CO_2 sensor (Vernier) and a commutator for EEG recordings (Pinnacle Technologies). The entire apparatus was maintained in a laboratory incubator (Isotemp 525D, Thermofisher) for temperature control. Temperatures used were targeted at 20°C, 32°C, and 42°C, and a 20-min exposure, unless mentioned otherwise, was initiated once the chamber recovered the desired temperature after the animal was placed into the chamber via an airlock. Gases were humidified and delivered at constant rates to the chamber. Room air or a custom gas mixture designed to mimic the nest environment (2.5% CO_2/21% O_2/76.5% N_2) was used to fill the chamber prior to animal entry. Observations of seizure behavior (rhythmic head movements with and without atypical vocalizations, clonus in two or more limbs, generalized convulsions with whole-body tonic-clonic activity, or movement arrest) were confirmed by an experimenter reviewing videos blinded to experimental conditions. In a subset of animals exposed to these environments, venous and mixed venous blood were collected following laceration of the saphenous vein or the right cardiac atrium after 20 min of exposure to these environments. Samples were collected within two min of exposure, after complete anesthesia with tribromoethanol (Avertin, 250 mg/kg, i.p.). Blood gas measures were made within three min of sample collection using a GEM Premier 4000 blood gas analyzer (Werferen) [60].

Patch clamp recordings from cortical pyramidal neurons

Two 12-month-old naked mole-rats and three postnatal day 16 mice (C57BL/6) were deeply anesthetized with tribromoethanol (Avertin, 125 mg/kg, i.p.) and transcardially perfused with 4°C sucrose-based slicing solution (in mM: 224 sucrose, 2.5 KCl, 0.5 $CaCl_2$, 7.0 $MgSO_4$, 1.25 NaH_2PO_4, 25 $NaHCO_3$, 25 D-glucose). The brain was removed and embedded in low melting point agarose. Coronal 400 μm-thick sections were cut using a Compresstome (Precisionary Instruments) and then incubated for one hour at 34°C in recording solution [72] (in mM: 124 NaCl, 3.5 KCl, 2 $CaCl_2$, 25 $NaHCO_3$, 1.1 NaH_2PO_4, 2 $MgSO_4$, and 10 mM D-glucose) bubbled with 95% O_2/5% CO_2 (carbogen).

Whole-cell voltage clamp and current clamp recordings were obtained using an EPC 10 patch clamp amplifier and Patchmaster software (both HEKA). Neocortical slices obtained from naked mole-rats and mice were maintained at 32°C in a heated chamber superfused at flow rate 3-3.5 ml/min with preheated carbogen-bubbled standard recording solution containing the following drugs: 10 μM bumetanide (to block Na-K-2Cl cotransport), 0.3 μM TTX, 1 μM CGP 55845, 10 μM CNQX, and 20 μM D-AP5 (all from Tocris) [72]. Pyramidal neurons were identified based on their morphology using a 40x water-immersion objective (Zeiss). Resting membrane potential was recorded upon entering whole-cell configuration in current clamp with zero current injection. To assess the efficacy of Cl^- extrusion mediated by KCC2 in pyramidal neurons of neocortical layer 2/3, a constant somatic Cl^- load (19 mM) was imposed on the neuron in whole-cell patch configuration via the recording pipette (4-5 MΩ bath resistance) filled with the following recording solution (in mM): 18 KCl, 111 K-gluconate, 0.5 $CaCl_2$, 2 NaOH, 10 glucose, 10 HEPES, 2 Mg-ATP, 5 BAPTA; pH adjusted to 7.3 with

KOH [72]. To assess E_{GABA} values in voltage clamp, $GABA_A$ receptor-mediated currents were elicited at varying holding potentials at a standardized dendritic location 50 μm away from the soma using pressure (18 psi; 10-20 ms) microinjection of 40 μM GABA (Tocris), dissolved in extracellular recording solution containing the above drugs, applied via a second glass capillary micropipette (tip diameter 2-3 μm) positioned close to the visually-traced apical dendrite of the same neuron. Membrane potential values were corrected for a calculated liquid junction potential of 14 mV.

Extracellular field recordings from hippocampal slices

Three adult naked mole-rats were deeply anesthetized with tribromoethanol (Avertin, 125 mg/kg, i.p.) and transcardially perfused with 4°C sucrose-based slicing solution (in mM: 252 sucrose, 5.0 KCl, 2.0 $CaCl_2$, 2.0 $MgSO_4$, 1.25 NaH_2PO_4, 26 $NaHCO_3$, 10 D-glucose). The brain was removed and embedded in low melting point agarose. Horizontal (400 μm) sections were cut through the ventral two-thirds of the hippocampus, using a Compresstome, and incubated for one to four hours where they were maintained at 32°C immersed in the above solution with sucrose now replaced by 126 mM NaCl (recording solution) and continuously bubbled with carbogen, pH 7.4. Following incubation, slices were placed in a Haas-type interface recording chamber (Scientific Systems Design), perfused with gravity-fed recording solution which was bubbled with carbogen, and warmed to 32°C. The slice surfaces were exposed to humidified carbogen. Extracellular recording electrodes made of borosilicate glass, pulled using a horizontal pipette puller (P-97, Sutter Instruments) to a 5-15 MΩ resistance, and filled with recording solution, were placed in the CA3 pyramidal cell layer. Data were amplified (ELC-03XS; NPI Electronic), and recorded on a computer running Igor Pro software (Wavemetrics) interfaced with an ITC-18 A/D board (Instrutech).

Spontaneous epileptiform bursts were identified as previously described in hippocampal slices from rats with spontaneous recurring seizures [69, 70] defined as a cluster of population spikes greater than 2 standard deviations from the root mean square amplitude of the trace. These events were nearly always present in the naked mole-rat CA3 pyramidal cell layer under typical recording conditions without electrical or chemical provocation. Once detected, burst activity was monitored for a minimum of 10 min prior to experimental manipulation. After a stable baseline recording was established, isoguvacine (200 μM) was added to the perfusate, and a 10-min recording was initiated. Recordings were imported into R and converted to time series using the IgorR package. Quantification of burst frequency, amplitude and power (line-length during the burst) was made using a moving window estimate of the standard deviation of the background activity and the findpeaks function of the Pracma package in R. Peak detection was set at three times the local standard deviation. Burst power was measured as the line-length of the trace divided by the duration of the burst event. Mean differences for burst amplitude, duration and power from baseline to isoguvacine were estimated using a paired sample Bayesian MCMC approach with default priors and Gibbs sampling in the Bayesian First Aid Package in R. Only results in which the 95% Highest Density Interval of the posterior distribution of the mean difference did not cross zero were considered significant.

QUANTIFICATION AND STATISTICAL ANALYSIS

Results in figures and text are reported as mean ± standard error of the mean, unless otherwise noted. Statistical analyses used are noted in the Results section and figure captions. The number of animals, neurons, or slices is indicated by n, with the appropriate unit indicated in the text.

DATA AND CODE AVAILABILITY

Datasets for the nest congregation and *in situ* gas infusion studies are available through the CUNY Academic Works server (with links provided in the Key Resources Table). Additional data files for electrophysiological experiments, and commands used in R and MATLAB for the preprocessing of behavioral and electrophysiological data are available from the Lead Contact upon request.